Phaseolus multiflorus var. albus

Subjects: Chemistry, Medicinal

Contributor: Ki Hyun Kim

Phaseolus multiflorus var. albus (Leguminosae), commonly known as "white kidney bean", is a twining perennial vine whose fruit has been used as a popular food worldwide owing to its high nutritional content, in terms of proteins, carbohydrates, fats, and vitamins.

Phaseolus multiflorus var. albus   Leguminosae   white kidney bean   denatonium

osteogenesis

1. Introduction

Phaseolus multiflorus var. *albus*, also known as white kidney bean, is a twining perennial vine belonging to the family Leguminosae. It has been cultivated for many purposes worldwide, especially in China [1]. Historically, leguminous plants have been popular worldwide because they are abundant in proteins (16–33%), minerals, carbohydrates, fats, vitamins, and phytoestrogens [1][2]. Pharmacological studies of plants belonging to the genus *Phaseolus* have reported that its extracts exhibit various therapeutic properties, including antidiabetic [1][2], antiobesogenic [3], antiproliferative [4], antioxidant, and gastroprotective activities [5]. In addition, previous studies on plants belonging to the genus *Phaseolus* have shown that their nutritional contents possess insecticidal, immunomodulatory, antitumor, and antifungal activities [4][5]. Previous biological studies on *P. multiflorus* var. *albus* reported that white kidney bean (*P. multiflorus* var. *albus*) treatments induced glucose reduction and weight loss in a diabetes-induced mouse model compared to the control group [6]. In this context, many clinical trials on the antiobesity effect of *P. multiflorus* var. *albus* have revealed that the ingestion of white kidney beans induces weight loss and waist circumference reduction [7]. In a recent study, *P. multiflorus* var. *albus* extract showed dose-dependent inhibitory activity against α-amylase [8]. Despite the health benefits of *P. multiflorus* var. *albus* extract, few studies have been carried out on its chemical constituents. Only a few previous phytochemical investigations of *P. multiflorus* have shown the presence of gibberellins A_1, A_5, A_6, A_8, and phaseic acid as plant hormones with growth-promoting activity [9][10][11][12].

Therefore, as part of our ongoing study to investigate novel bioactive components from various natural resources [13][14][15][16][17][18][19], we investigated the potential bioactive components from the extract of *P. multiflorus* var. *albus* fruits. In the current study, the phytochemical constituents of the ethanolic extract of *P. multiflorus* var. *albus* fruits were isolated, resulting in the isolation of three phenolic compounds (**1–3**) and one dipeptide (**4**). The chemical structures of compounds (**1–4**) were clearly elucidated through 1D and 2D nuclear magnetic resonance (NMR) spectroscopic data and high-resolution electrospray ionization (HR-ESI) liquid

chromatography–mass spectrometry (LC/MS) analyses. In addition, the isolated compounds, **1–4,** were tested for their regulatory effects on the differentiation between osteogenesis and adipogenesis of mesenchymal stem cells (MSCs). Herein, we report the isolation and structural determination of the isolated compounds **1–4** as well as their regulatory effects on the differentiation of MSCs.

2. Isolation of Compounds

The fruits of *P. multiflorus* var. *albus* were extracted with 30% ethanol/H_2O. The resultant extract was suspended for solvent partitioning in water and then fractionated with four solvents, which afforded hexane-soluble (31.4 mg), dichloromethane-soluble (195.7 mg), ethyl acetate-soluble (49.3 mg), and *n*-butanol-soluble (2.4 g) fractions. The LC/MS-based analysis combined with our in-house built UV library and thin-layer chromatography (TLC) analysis of the solvent-partitioned fractions suggested that the BuOH-soluble fraction contained the majority of the organic acid derivatives. A phytochemical investigation of the solvent-partitioned fractions was conducted under monitoring by TLC and LC/MS-based analysis using repeated column chromatography with silica gel 60, RP-C_{18} silica gel, and Sephadex LH-20, and high-performance liquid chromatography (HPLC) (**Figure 1**). The final semi-preparative HPLC separation afforded a phenolic compound (**1**) from the EA-soluble fraction, two phenolic compounds (**2** and **3**) from the hexane-soluble fraction, and one dipeptide (**4**) from the *n*-butanol-soluble fraction (**Figure 2**).
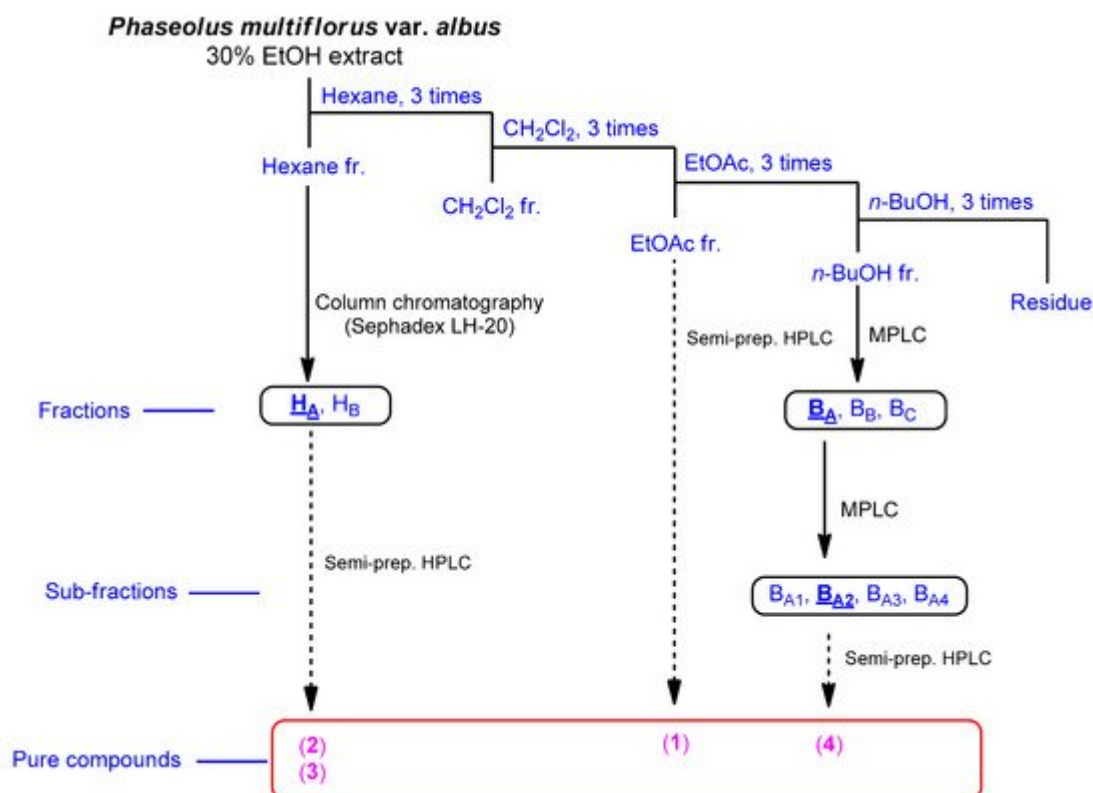

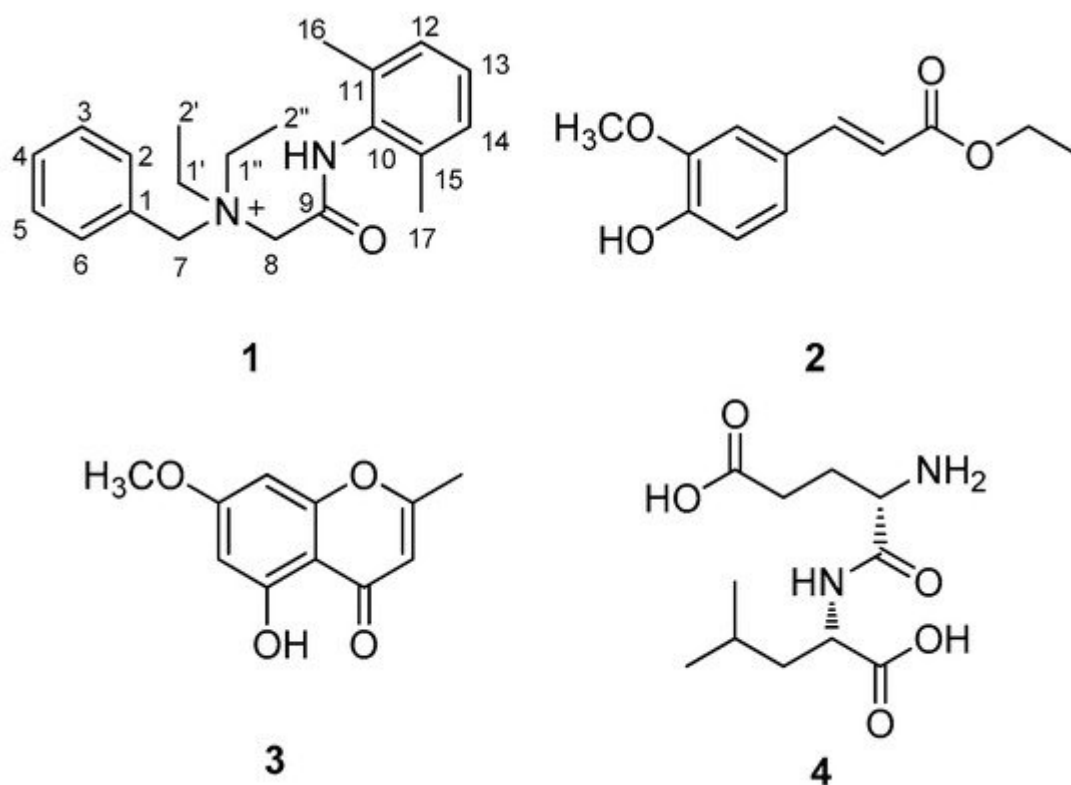**Figure 1.** Separation scheme of compounds **1–4**.

Figure 2. Chemical structures of compounds **1–4**.

3. Elucidation of Compound Structures

Compound **1** was isolated as a white amorphous powder. The molecular formula was deduced to be $C_{21}H_{29}N_2O^+$ from the molecular ion peak $[M]^+$ at *m/z* 325.2282 (calculated for $C_{21}H_{29}N_2O^+$, 325.2274) in the positive-ion mode of HRESIMS (Figure S1). The ^1H NMR spectrum of **1** (**Table 1**, Figure S2) displayed the presence of the characteristic signals of two aromatic proton sets of a monosubstituted aromatic ring at δ_H 7.64 (2H, t, *J* = 7.5 Hz), δ_H 7.62 (1H, t, *J* = 7.5 Hz), and δ_H 7.58 (2H, t, *J* = 7.5 Hz); 1,2,6-trisubstituted aromatic ring at δ_H 7.18 (1H, t, *J* = 7.0 Hz) and δ_H 7.17 (2H, d, *J* = 7.0 Hz); two pairs of relatively deshielded methylene groups at δ_H 4.94 (2H, s) and δ_H 4.16 (2H, s); two symmetric methyl groups at δ_H 2.30 (6H, s); and another two pairs of ethyl groups at δ_H 3.67 (4H, m) and δ_H 1.56 (6H, t, *J* = 7.5 Hz). The ^{13}C NMR data of **1** (**Table 1**, Figure S3), assigned with the aid of the HSQC (Figure S5) and HMBC experiments (Figure S6)confirmed 21 carbon signals composed of four methyl groups at δ_C 8.4 (2 × C) and δ_C 18.7 (2 × C); four methylene carbons at δ_C 54.9 (2 × C), δ_C 55.7, and δ_C 63.4; 12 aromatic carbons (δ_C 128.7, 129.1, 129.5 (2 × C), 130.7 (2 × C), 132.3, 134.1 (2 × C), 134.2, 136.7 (2 × C)); and a carbonyl carbon at δ_C 164.1. The partial structures of **1** were determined by 2D NMR experiments (^1H-^1H COSY and HMBC). The gross structure of **1** was finally elucidated by the characteristic NMR signals, and its molecular formula ($C_{21}H_{29}N_2O^+$) was confirmed by HRESIMS. The ^1H-^1H COSY correlations (Figure S4) between H-2/H-3/H-4/H-5/H-6 as well as the HMBC correlations of H-2(H-6)/C-7 (δ_C 63.4) and H_2-7/C-1, C-2, and C-3 verified the presence of benzyl functionality (**Figure 3**). Furthermore, the methylene of H_2-7 showed HMBC correlations with three other carbons: C-8 (δ_C 55.7), C-1′ (δ_C 54.9), and C-1″ (δ_C 54.9) (**Figure 3**),

providing evidence that a quaternary atom linking C-7, C-8, C-1′, and C-1″ is present. Based on the ^{1}H-^{1}H COSY spectrum of H$_2$-1′/H$_2$-2′ and H$_2$-1″/H$_2$-2″ and the HMBC correlations of H$_2$-1′/H$_2$-1″ with C-2′/C-2″, along with their symmetric NMR signals, the two ethyl units were assigned and confirmed to be attached to the quaternary atom by the HMBC correlations of H$_2$-1′/H$_2$-1″ with C-7 and C-8. The relatively deshielded methylene carbon NMR signals of C-7, C-8, C-1′, and C-1″ and the markedly diminished intensity of the carbon NMR signals observed for C-1′, and C-1″ at δ_C 54.9 confirmed that the quaternary atom linking them could be a quaternary ammonium cation, which finally led to the partial structure of A (**Figure 3**). Another spin system was observed as a cross-peak between H-12/H-13/H-14 in the ^{1}H-^{1}H COSY spectrum, representing the 1,2,6-trisubstituted aromatic ring, which was assigned to the 2,6-dimethylated benzene as the partial structure of B by the HMBC correlations of H-12(H-14)/C-10, H-13/C-11(C-15), C-16(C-17)/C-10, C-11, and C-12 (**Figure 3**). Finally, the connectivity through the amide bond between the two partial structures of A and B was suggested by the C=O and NH moieties remaining from the molecular formula (C$_{21}$H$_{29}$N$_2$O$^+$) of **1**, the detected HMBC correlation of H$_2$-8/C-9 (δ_C 164.1), and the characteristic ^{13}C chemical shifts of C-8 (δ_C 55.7) and C-10 (δ_C 134.2), although the key HMBC correlation between C-9 and C-10 was missing in **1** due to the absence of protons. Accordingly, the complete structure of **1** was established, as shown in **Figure 1**, and it was identified to be denatonium.
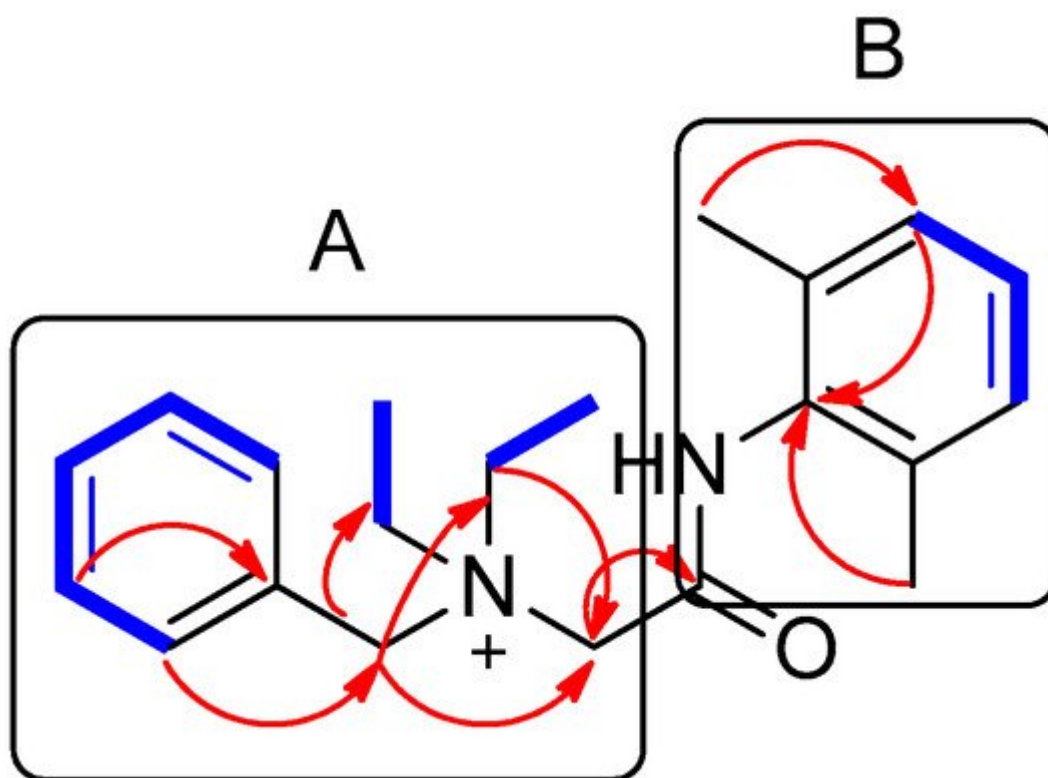

Figure 3. Key ^{1}H-^{1}H COSY (▬) and HMBC (⌒) correlations of compound **1**. A and B represent two partial structures.

Table 1. ^{1}H and ^{13}C NMR data of compound **1** in CD$_3$OD (δ in ppm, 850 MHz and 212.5 MHz for ^{1}H and ^{13}C, respectively) ^{a}.

Position	Denatonium (1)	
	δ_H (*J* in Hz)	δ_C
1		128.7 C
2	7.64, d (7.5)	134.1 CH
3	7.58, t (7.5)	130.7 CH
4	7.62, t (7.5)	132.3 CH
5	7.58, t (7.5)	130.7 CH
6	7.64, d (7.5)	134.1 CH
7	4.94, s	63.4 CH_2
8	4.16, s	55.7 CH_2
9		164.1 C
10		134.2 C
11		136.7 C
12	7.17, d (7.0)	129.5 CH
13	7.18, t (7.0)	129.1 CH
14	7.17, d (7.0)	129.5 CH
15		136.7 C
16	2.30, s	18.7 CH_3
17	2.30, s	18.7 CH_3
1′	3.67, m	54.9 CH_2
2′	1.56, t (7.5)	8.4 CH_3
1″	3.67, m	54.9 CH_2
2″	1.56, t (7.5)	8.4 CH_3

er (**2**) [20], eugenin (**3**) [21], and α-L-glutamyl-L-Leucine (**4**) [22] by comparing their NMR spectroscopic data with those previously reported in the literature and MS data obtained from the LC/MS analysis. To the best of our knowledge, denatonium (**1**) was identified from a natural source for the first time, and compounds **2–4** were reported for the first time from *P. multiflorus* var. *albus* in this study. In natural product chemistry, it is important to take the

^a Coupling constants (Hz) are given in parentheses. ¹³C NMR assignments were based on HSQC, ¹H-¹H COSY, necessary precautions during the isolation work in order to minimize the possibility of unexpected artifact isolation and HMBC experiments.

[23]. To verify whether compounds **1–4** were genuine natural compounds or artifacts, *P. multiflorus* var. *albus* was extracted with 80% methanol (*v/v*) for 10 h, and the resultant methanolic extract was subjected to LC/MS analysis. As a result, there was no peak with a molecular ion corresponding to compound **2** in the methanolic extract, whereas compounds **1**, **3**, and **4** were detected, suggesting that compound **2** was an artifact produced by the

extraction with ethanol. In addition, to confirm that the isolated denatonium (**1**) is a natural compound, the methanol used for extraction was analyzed using ultra-performance liquid chromatography (UPLC) quadrupole time-of-flight (Q-TOF) high-resolution (HR)-MS because methanol can possess denatonium as a component. As a result, there was no detected peak for denatonium in the methanol solvent that we used for extraction (Figure S7), suggesting that the methanol used does not contain denatonium and the isolated denatonium can be a genuine natural compound.

Intriguingly, denatonium (benzyl-[2-(2,6-dimethylanilino)-2-oxoethyl]-diethylazanium), which is odorless and chemically stable, was found during research on local anesthetics in 1958 [24]. Since then, it has been widely used in various industries, such as cosmetics, pharmaceuticals, and material industries [25]. Interestingly, its bitterness and aversive taste have served to prevent young children from swallowing small household items, including toys and game packs, which has allowed denatonium to be widely employed in many household items. Denatonium is known to be one of the most bitter chemical compounds; thus, it was nominated in the Guinness Book of World Records as one of the most bitter compounds that people can use [26].

4. Evaluation of the Biological Activities of Compounds *1–4*

MSCs are pluripotent cells in bone marrow that are known to differentiate into osteocytes and adipocytes. As microenvironmental changes cause alterations in the regulation of gene expression in MSC differentiation, the alterations of related gene expression might disturb the balance between adipocyte progenitor and osteoprogenitor cells in patients with osteoporosis [27][28][29]. Thus, a therapy that can regulate gene expression in MSCs would be promising for the management of postmenopausal osteoporosis. To determine the regulatory effects of compounds **1–4** on MSC differentiation between adipogenesis and osteogenesis, all the compounds were examined for their effects on the differentiation of murine MSCs into adipocytes or osteoblasts. The murine MSC line C3H10T1/2 was treated with 20 µM of the compounds during adipogenesis, and the differentiated cells were stained with Oil Red O (ORO). Compound **4** slightly reduced the formation of lipid droplets, resulting in fewer ORO-stained cells, compared to the normally differentiated adipocytes (**Figure 4**A,B). In addition, C3H10T1/2 cells were cultured in osteogenesis-inducing media in the presence of compounds **1–4**. The cells were then stained for alkaline phosphatase (ALP), which is considered a distinctive marker of osteoblast differentiation [30]. Cells treated with compounds **1** and **4** showed slightly higher staining intensity and ALP enzyme activity than the negative control group (**Figure 4**C,D).
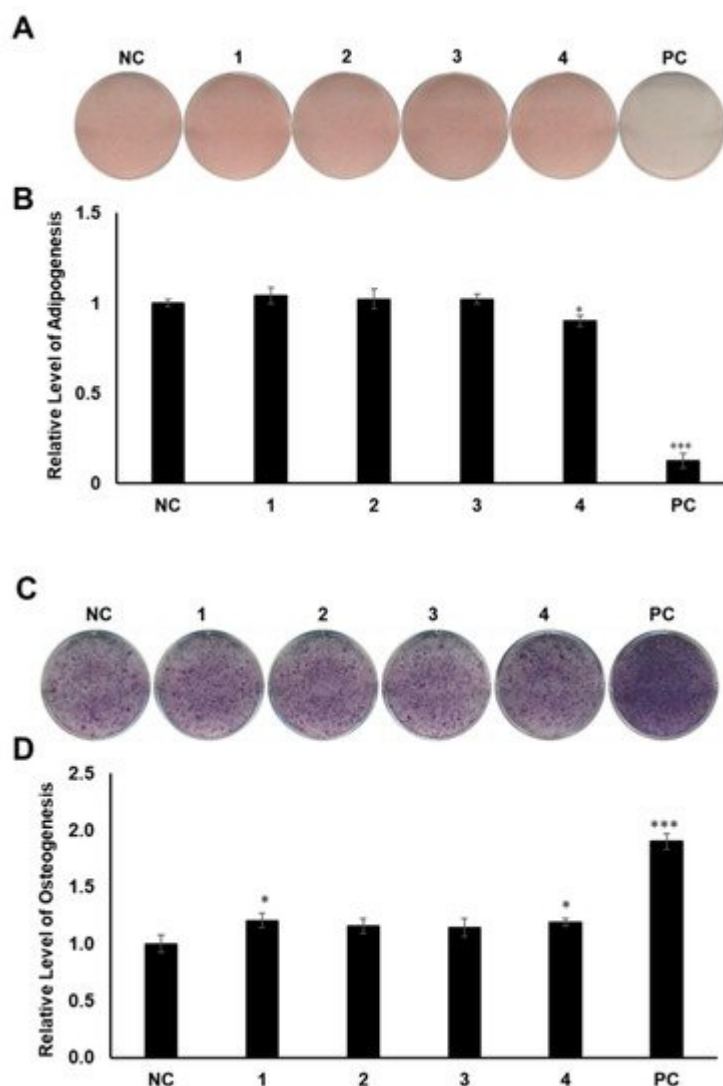
Figure 4. The effects of compounds **1–4** on the differentiation of mesenchymal stem cells (MSCs) toward adipocytes and osteoblasts. (**A**) Suppressive effects of compounds **1–4** on the adipogenic differentiation of MSCs. C3H10T1/2 cells were treated with 20 μM of compounds **1–4**. After adipogenic differentiation, the cells were stained with Oil Red O (ORO). (**B**) The intensity of stained lipid droplets was quantitatively examined. (**C**) Stimulatory effects of compounds **1–4** on osteogenic differentiation of MSCs. Fully differentiated C3H10T1/2 cells were stained with alkaline phosphatase (ALP) on day 9 post osteogenic differentiation with 20 μM compounds **1–4**. (**D**) ALP enzyme activity was determined in osteogenically differentiated C3H10T1/2 cells treated with compounds **1–4**. The values were calculated relatively by setting the untreated negative control (NC) to 1. Resveratrol (20 μM) and oryzativol A (5 μM) were added to the experimental set for adipogenesis and osteogenesis, respectively, as a positive control (PC). * denotes $p < 0.05$ and *** denotes $p < 0.001$.

Compounds **1** and **4** showed the regulatory effects on the differentiation between osteogenesis and adipogenesis of MSCs (**Figure 4**). Among the active compounds, compound **4** was not sufficient for further experiments to examine its effects. To test the effects of compound **1** on osteogenic differentiation, C3H10T1/2 cells were stained with ALP (**Figure 5**A), and ALP enzyme activity was measured (**Figure 5**B). Our results indicated that increased concentrations of compound **1** led to the formation of darker-colored cells (**Figure 5**A), which indicated that the

treated cells exhibited greater promotion of bone differentiation than the control group (**Figure 5**B). Moreover, compound **1** slightly enhanced the gene expression of *ALP* (**Figure 5**C) and osteopontin (*OPN*) (**Figure 5**D), which are osteogenesis-related factors, during osteogenic differentiation in a dose-dependent manner.
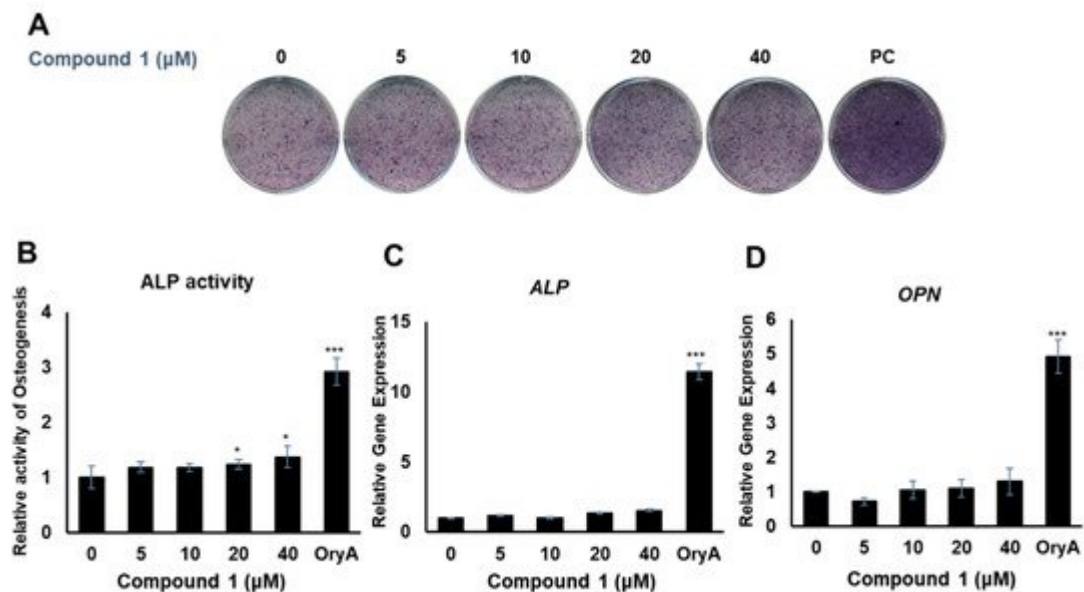

Figure 5. The effects of compound **1** on osteogenic differentiation. C3H10T1/2 cells were treated with sequential concentrations (5, 10, 20, and 40 μM) of compound **1** during osteogenic differentiation. The effects of compound **1** were evaluated through ALP staining (**A**). The cells were evaluated by measuring the ALP activity (**B**). The mRNA expression of *ALP* (**C**) and *OPN* (**D**) was measured by real-time PCR. Oryzativol A (OryA) at a concentration of 5 μM was used as a positive control (PC). * denotes $0.01 < p < 0.05$ and *** denotes $p < 0.001$.

References

1. Meng, J.; Bai, Z.; Huang, W.; Liu, Y.; Wang, P.; Nie, S.; Huang, X. Polysaccharide from white kidney bean can improve hyperglycemia and hyperlipidemia in diabetic rats. Bioact. Carbohydr. Diet. Fibre 2020, 24, 100222.

2. Mojica, L.; de Mejía, E.G. Characterization and comparison of protein and peptide profiles and their biological activities of improved common bean cultivars (Phaseolus vulgaris L.) from Mexico and Brazil. Plant Foods Hum. Nutr. 2015, 70, 105–112.

3. Neil, E.S.; McGinley, J.N.; Fitzgerald, V.K.; Lauck, C.A.; Tabke, J.A.; Streeter-McDonald, M.R.; Yao, L.; Broeckling, C.D.; Weir, T.L.; Foster, M.T. White kidney bean (Phaseolus Vulgaris L.) consumption reduces fat accumulation in a polygenic mouse model of obesity. Nutrients 2019, 11, 2780.

4. Li, M.; Liu, Q.; Cui, Y.; Li, D.; Wang, H.; Ng, T.B. Isolation and characterization of a Phaseolus vulgaris trypsin inhibitor with antiproliferative activity on leukemia and lymphoma cells. Molecules

2017, 22, 187.

5. E Lacerda, R.R.; do Nascimento, E.S.; de Lacerda, J.T.J.G.; da Silva Pinto, L.; Rizzi, C.; Bezerra, M.M.; Pinto, I.R.; Pereira Filho, S.M.; Pinto, V.d.P.T.; Cristino Filho, G. Lectin from seeds of a Brazilian lima bean variety (Phaseolus lunatus L. var. cascavel) presents antioxidant, antitumour and gastroprotective activities. Int. J. Biol. Macromol. 2017, 95, 1072–1081.

6. Jabir, A.S.; Iraby, A.G. Studying the effect of anti-amylase inhibitor extracted from white kidney bean (Phaseolus vulgaris) in treat diabetes and obesity in an affected mice. Int. J. Curr. Microbiol. App. Sci 2014, 3, 97–106.

7. Barrett, M.L.; Udani, J.K. A proprietary alpha-amylase inhibitor from white bean (Phaseolus vulgaris): A review of clinical studies on weight loss and glycemic control. Nutr. J. 2011, 10, 1–10.

8. Kim, D.H.; Park, Y.H.; Lee, J.S.; Jeong, H.I.; Lee, K.W.; Kang, T.H. Anti-obesity effect of DKB-117 through the inhibition of pancreatic lipase and α-amylase activity. Nutrients 2020, 12, 3053.

9. MacMillan, J.; Pryce, R. Further investigations of gibberellins in Phaseolus multiflorus by combined gas chromatography-mass spectrometry-the occurence of gibberellin A20 (pharbitis gibberellin) and the structure of compound b. Tetrahedron Lett. 1968, 9, 1537–1542.

10. MacMillan, J.; Seaton, J.; Suter, P. Plant hormones—I: Isolation of gibberellin A1 and gibberellin A5 from Phaseolus multiflorus. Tetrahedron 1960, 11, 60–66.

11. MacMillan, J.; Pryce, R. Plant hormones—IX: Phaseic acid, a relative of abscisic acid from seed of Phaseolus multiflorus. Possible structures. Tetrahedron 1969, 25, 5893–5901.

12. MacMillan, J.; Suter, P. The structure of a C12-acid from the seed of Phaseolus multiflorus. Tetrahedron 1967, 23, 2417–2419.

13. Lee, S.R.; Kang, H.; Yoo, M.J.; Yu, J.S.; Lee, S.; Yi, S.A.; Beemelmanns, C.; Lee, J.; Kim, K.H. Anti-adipogenic pregnane steroid from a Hydractinia-associated fungus, Cladosporium sphaerospermum SW67. Nat. Prod. Sci. 2020, 26, 230–235.

14. Yu, J.S.; Park, M.; Pang, C.; Rashan, L.; Jung, W.H.; Kim, K.H. Antifungal phenols from Woodfordia uniflora collected in Oman. J. Nat. Prod. 2020, 83, 2261–2268.

15. Lee, S.; Lee, D.; Ryoo, R.; Kim, J.-C.; Park, H.B.; Kang, K.S.; Kim, K.H. Calvatianone, a sterol possessing a 6/5/6/5-fused ring system with a contracted tetrahydrofuran B-ring, from the fruiting bodies of Calvatia nipponica. J. Nat. Prod. 2020, 83, 2737–2742.

16. Trinh, T.A.; Park, E.-J.; Lee, D.; Song, J.H.; Lee, H.L.; Kim, K.H.; Kim, Y.; Jung, K.; Kang, K.S.; Yoo, J.-E. Estrogenic activity of sanguiin H-6 through activation of estrogen receptor α coactivator-binding site. Nat. Prod. Sci. 2019, 25, 28–33.

17. Yu, J.S.; Li, C.; Kwon, M.; Oh, T.; Lee, T.H.; Kim, D.H.; Ahn, J.S.; Ko, S.-K.; Kim, C.S.; Cao, S. Herqueilenone A, a unique rearranged benzoquinone-chromanone from the hawaiian volcanic

soil-associated fungal strain Penicillium herquei FT729. Bioorg. Chem. 2020, 105, 104397.

18. Ha, J.W.; Kim, J.; Kim, H.; Jang, W.; Kim, K.H. Mushrooms: An important source of natural bioactive compounds. Nat. Prod. Sci. 2020, 26, 118–131.

19. Lee, S.; Ryoo, R.; Choi, J.H.; Kim, J.-H.; Kim, S.-H.; Kim, K.H. Trichothecene and tremulane sesquiterpenes from a hallucinogenic mushroom Gymnopilus junonius and their cytotoxicity. Arch. Pharm. Res. 2020, 43, 214–223.

20. Bolling, B.W.; Parkin, K.L. Phenolic derivatives from soy flour ethanol extract are potent in vitro quinone reductase (QR) inducing agents. J. Agric. Food Chem. 2008, 56, 10473–10480.

21. Ali, A.; Makboul, M.; Attia, A.; Ali, D. Chromones and flavans from Pancratium maritimum. Phytochemistry 1990, 29, 625–627.

22. Kasai, T.; Sakamura, S. NMR spectra of glutamic acid-containing dipeptides in relation to sequence determination. Agric. Biol. Chem. 1973, 37, 2155–2157.

23. Venditti, A. What is and what should never be: Artifacts, improbable phytochemicals, contaminants and natural products. Nat. Prod. Res. 2020, 34, 1014–1031.

24. What is Bitrex? Available online: https://www.bitrex.com/about-bitrex/what-is-bitrex (accessed on 3 October 2021).

25. Kwiatkowski, A.; Czerwicka, M.; Smulko, J.; Stepnowski, P. Detection of denatonium benzoate (Bitrex) remnants in noncommercial alcoholic beverages by raman spectroscopy. J. Forensic Sci. 2014, 59, 1358–1363.

26. Sibert, J.R.; Frude, N. Bittering agents in the prevention of accidental poisoning: children's reactions to denatonium benzoate (Bitrex). Arch. Emerg. Med. 1991, 8, 1–7.

27. Meyer, M.B.; Benkusky, N.A.; Sen, B.; Rubin, J.; Pike, J.W. Epigenetic plasticity drives adipogenic and osteogenic differentiation of marrow-derived mesenchymal stem cells. J. Biol. Chem. 2016, 291, 17829–17847.

28. Yi, S.A.; Lee, J.; Park, S.K.; Kim, J.Y.; Park, J.W.; Lee, M.G.; Nam, K.H.; Park, J.H.; Oh, H.; Kim, S. Fermented ginseng extract, BST204, disturbs adipogenesis of mesenchymal stem cells through inhibition of S6 kinase 1 signaling. J. Ginseng Res. 2020, 44, 58–66.

29. Ciuffreda, M.C.; Malpasso, G.; Musarò, P.; Turco, V.; Gnecchi, M. Protocols for in vitro differentiation of human mesenchymal stem cells into osteogenic, chondrogenic and adipogenic lineages. In Mesenchymal Stem Cells; Springer: New York, NY, USA, 2016; pp. 149–158.

30. Kang, M.-H.; Lee, S.-J.; Lee, M.-H. Bone remodeling effects of Korean Red Ginseng extracts for dental implant applications. J. Ginseng Res. 2020, 44, 823–832.